

The Optimal Spacing between Elliptic Tubes Cooled by Free Convection Using Constructal Theory

Ahmed Waheed Mustafa

Mechanical Eng. Dep., Coll. of Engineering, AL-Nahrain University
ahmedwah@eng.nahrainuniv.edu.iq

Jaafar Ahmed Zahi

Mechanical Eng. Dep., Coll. of Engineering, AL-Nahrain University
jafaralkhafajy@gmail.com

Abstract:

The optimal spacing between elliptic tubes cooled by free convection is studied numerically. A row of isothermal elliptic tubes are installed in a fixed volume and the spacing between them is selected according to the constructal theory (Bejan's theory). In this theory the spacing between the tubes is chosen such that the heat transfer density is maximized. A finite volume method is employed to solve the governing equations; SIMPLE algorithm with collocated grid is utilized for coupling between velocity and pressure. The range of Rayleigh number is ($10^3 \leq Ra \leq 10^5$), the range of the axis ratio of the tubes is ($0 \leq \varepsilon \leq 0.5$), and the working fluid is air ($Pr = 0.71$). The results show that the optimal spacing decreases as Rayleigh number increases for all axis ratios, and the maximum density of heat transfer increases as the Rayleigh number increases for all axis ratios and the highest value occurs at axis ratio ($\varepsilon = 0$) (flat plate) while the lowest value occurs at ($\varepsilon = 0.5$) (circular tube). The results also show that the optimal spacing is unchanged with the axis ratio at constant Rayleigh number.

Keywords: Constructal theory, optimal spacing, elliptic tubes, natural convection

Nomenclature

a	Major axis of the tube (m)
b	Minor axis of the tube (m)
d	Height of the tube = $2a$ (m)
D	Non-dimensional height of the tube
g	Gravity acceleration (m/s^2)
H_d	Dimensionless downstream extension
H_u	Dimensionless upstream extension
k	Thermal conductivity (W/m.k)
L	Total length of the domain (m)
p	Pressure (N/m^2)
P	Non-dimensional pressure
Pr	Prandtl number
q	Heat transfer rate (W)
Q	Dimensionless heat transfer density
Ra	Rayleigh number
s	Spacing between the tubes (m)
S	Dimensionless Spacing
t	Temperature ($^{\circ}C$)
T	Dimensionless temperature

T_w	Wall temperature ($^{\circ}C$)
T_{∞}	Ambient temperature ($^{\circ}C$)
u	Horizontal velocity (m/s)
U	Dimensionless horizontal velocity
v	Vertical velocity (m/s)
V	Dimensionless vertical velocity
V	Volume (m^3)
w	Width (m)
x	Horizontal Coordinate (m)
X	Dimensionless Horizontal Coordinate
y	Vertical coordinate (m)
Y	Dimensionless vertical coordinate

Greek Symbols

α	Thermal diffusivity (m^2/s)
β	Coefficient of thermal expansion (K^{-1})
ε	Axis ratio
ρ	Density (Kg/m^3)
ν	Kinematic viscosity (Pa.s)

Subscripts

Max	Maximum value
Opt	Optimum value

1. Introduction

In heat transfer, constructal theory (Bejan's theory) is used to generate the flow configuration by optimizing the heat transfer density under (space) volume constraint. Constructal theory states that the flow configuration is free to morph in the follow-up of maximal global performance (objective function) under global constraints, Bejan A. and Lorente S., (2008), [1]. By depending on constructal theory, the optimal spacing between plates and cylinders cooled by natural convection can be found, in each geometry, the total volume is fixed and the objective is to maximize the overall thermal conductance between the tubes. Bejan A., (1984), [2] found the optimal spacing between vertical plates installed in a fixed volume by using the intersecting of asymptotes method. The study was employed for isothermal vertical plates cooled by natural convection. He found that the optimal spacing was proportional to the Rayleigh number to the power of (-1/4). Bejan A. et al. (1995), [3] carried out a numerical and experimental study of how to choose the spacing among horizontal cylinders installed in

a fixed volume cooled by laminar free convection. They maximized the total density of heat transfer between the assembly and the ambient. The Numerical and experimental simulations cover the Rayleigh number range of $10^4 \leq Ra \leq 10^7$ and $Pr = 0.72$. Ledezma G. A. and Bejan A., (1997), [4] investigated numerically and experimentally the free convection from staggered vertical plates installed in fixed space. They maximized the density of heat transfer and they considered three degrees of freedom; the horizontal spacing between adjacent columns, the stagger between columns and the plate dimensions. Numerical and experimental simulations cover the Rayleigh number range of $10^3 \leq Ra \leq 10^6$, and the working fluid was air with $Pr=0.72$. The conclusion demonstrated numerically and experimentally that it was possible to optimize geometrically the internal architecture of a fixed volume such that its global thermal resistance was minimized. Da Silva and A. Bejan, (2004), [5] studied numerically the free convection in vertical converging or diverging channel with optimized for density of heat transfer. They considered three degrees of freedom: the distribution of heat on the wall, wall to wall spacing, and the angle between the two walls. The optimization was performed in the range of $10^5 \leq Ra \leq 10^7$ and $Pr=0.7$. The walls were partially heated either at top of the channel or at the bottom of the channel. They proved that the density of heat transfer increased by putting the unheated part at the upper sections. They also showed that the best angle among the walls was almost zero when Ra number was high. Da Silva A. K. and Bejan A., (2005), [6] designed numerically a multi-scale plates geometry cooled by free convection by using constructal theory. They maximized the density of heat transfer rate. They put small plates in the unused heat transfer area between the large plates. They used finite element method to discretize the governing equation in the range of Rayleigh number of $10^5 \leq Ra \leq 10^8$, and $Pr= 0.7$. They showed that the density of heat transfer increased by putting the small plates between the large plates. Da Silva A.K. et al. (2005), [7] studied the free convection from discrete heat sources placed in vertical open channel with the constructal theory. They considered two cases, the first was single heat source under variable size, and the second was heat sources with fixed size. They applied the constructal theory to maximize the thermal conductance between the cold air and the discrete heat sources or to minimize the hot spot on the hot sources. Rayleigh number was in the range of $(10^2 \leq Ra \leq 10^4)$ and $Pr = 0.7$. They showed

that for case one the thermal performance can be maximized as the heat source not covering the entire wall at $Ra = 10^2$ and 10^3 . Bello-Ochende T. and Bejan A., (2005), [8] designed numerically a multi-scale cylinders geometry cooled by free convection by using constructal theory. They maximized the density of heat transfer rate. They put small cylinders in the unused heat transfer area between the large cylinders. They used finite element method to discretize the governing equation in the range of Rayleigh number of $10^5 \leq Ra \leq 10^8$, and $Pr= 0.7$. They showed that the density of heat transfer increased by putting the small cylinders between the large cylinders. Page L. et al., (2011), [9] investigated numerically the free convection from single scale rotating cylinders. They used the constructal theory to maximize the density of heat transfer rate. The range of Rayleigh number was $(10^1 \leq Ra \leq 10^4)$, the range of rotating speed was $(0 \leq \tilde{\omega}_0 \leq 10)$, and the fluid was air ($Pr=0.7$). They found that the optimized spacing decreases as Rayleigh number increases and the heat transfer density increases. Page L. et al. (2013), [10] investigated numerically the free convection from multi-scales rotating cylinders. They used constructal theory in order to find the optimal arrangement of the geometry. The range of Rayleigh number was $(10^2 \leq Ra \leq 10^4)$, the range of rotating speed was $(0 \leq \tilde{\omega}_0 \leq 10)$, and the fluid was air ($Pr=0.7$). Small cylinders were put in the unused regions of heat transfer. They found that there were no effects of the rotating cylinders on heat transfer density in compare with the stationary cylinders except at high speeds of rotation.

It is obvious from the literature that there is no attempt to find the optimal spacing between elliptic tubes cooled by natural convection with constructal theory, so that the present study uses the constructal theory to find the spacing numerically.

2. Mathematical Model

Consider a row of elliptic tubes installed in a fixed volume per unit depth (dL) as shown in figure (1). The major axis of the elliptic tube is ($a = d/2$), the minor axis of the tube is (b). The axis ratio is defined as ($\varepsilon = b/d$). The tubes are maintained at constant wall (hot) temperature of (T_w), the ambient temperature is maintained at constant temperature of (T_∞). The objective is to find the number of tubes or the tube – to – tube spacing (s) for different axis ratio (ε) in order to maximize the heat transfer density. Therefore there are two degrees of freedom in this geometry, the first is the spacing (s) and the second is the axis ratio

(ε). The dimensionless governing equations for steady, laminar, and incompressible flow with Boussinesq approximation for the density in the buoyancy term can be written as ; Zhang Z. et al. (1991), [11]

$$\frac{\partial U}{\partial X} + \frac{\partial V}{\partial Y} = 0 \tag{1}$$

$$\left(U \frac{\partial U}{\partial X} + V \frac{\partial U}{\partial Y} \right) = -\frac{\partial P}{\partial X} + \left(\frac{Pr}{Ra} \right)^{1/2} \left(\frac{\partial^2 U}{\partial X^2} + \frac{\partial^2 U}{\partial Y^2} \right) \tag{2}$$

$$\left(U \frac{\partial V}{\partial X} + V \frac{\partial V}{\partial Y} \right) = -\frac{\partial P}{\partial Y} + \left(\frac{Pr}{Ra} \right)^{1/2} \left(\frac{\partial^2 V}{\partial X^2} + \frac{\partial^2 V}{\partial Y^2} \right) + T \tag{3}$$

$$\left(U \frac{\partial T}{\partial X} + V \frac{\partial T}{\partial Y} \right) = \frac{1}{(Ra Pr)^{1/2}} \left(\frac{\partial^2 T}{\partial X^2} + \frac{\partial^2 T}{\partial Y^2} \right) \tag{4}$$

The non-dimensionalised variables and groups used are;

$$X = \frac{x}{d}, \quad Y = \frac{y}{d}, \quad U = \frac{u}{\left(\frac{\alpha}{d} \right) (Ra Pr)^{1/2}}$$

$$V = \frac{v}{\left(\frac{\alpha}{d} \right) (Ra Pr)^{1/2}}, \quad P = \frac{Pd^2}{\alpha^2 \rho Ra Pr}, \quad T = \frac{t - T_\infty}{T_w - T_\infty}$$

$$Pr = \frac{\nu}{\alpha},$$

$$Ra = \frac{g \beta d^3 (T_w - T_\infty)}{\alpha \nu} \tag{5}$$

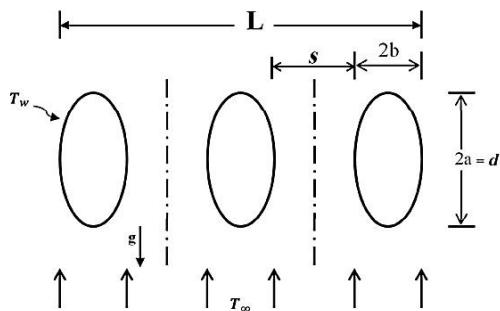


Figure (1): Physical Geometry of the Present Problem

Since the flow is symmetrical between the tubes, only half of the flow channel between two tubes can be used to find the spacing in the numerical solution. Half of the flow channel is shown in figure (2). The total height of the channel is ($H_u + D + H_d$), the upstream height (H_u) and downstream (H_d) are added to avoid the applying of incorrect velocity and temperature at the inlet and outlet of the

channel, these extension (H_u, H_d) are selected according to accuracy tests as shown later.

The flow and thermal dimensionless boundary conditions on the half channel are shown in figure (2) and can be summarized as;

Tube surfaces ($H_u \leq Y \leq D$) (no slip and no penetration and constant wall temperature $U = V = 0, T = 1$)

Channel Inlet ($0 \leq X \leq \left(\frac{s}{2} + \varepsilon \right)$)

$$\left(U = \frac{\partial V}{\partial Y} = 0, T = 0, P = 0 \right)$$

Channel exit ($0 \leq X \leq \left(\frac{s}{2} + \varepsilon \right)$)

$$\left(\frac{\partial(U, V, T)}{\partial Y} = 0, P = 0 \right)$$

Left and right sides of the upstream section

($0 \leq Y \leq H_u$) (free slip and no penetration

$$U = \frac{\partial V}{\partial X} = 0, \frac{\partial P}{\partial X} = 0, \frac{\partial T}{\partial X} = 0)$$

Left side of the downstream section

($H_u + D \leq Y \leq H_u + D + H_d$) (free slip and

$$\text{no penetration } U = \frac{\partial V}{\partial X} = 0, \frac{\partial P}{\partial X} = 0, \frac{\partial T}{\partial X} = 0)$$

Right side of the downstream section

($H_u + D \leq Y \leq H_u + D + H_d$) (zero stress

$$\frac{\partial(V, U)}{\partial X} = 0, \frac{\partial P}{\partial X} = 0, \frac{\partial T}{\partial X} = 0)$$

The right side of the downstream boundary condition is applied to permit fluid to enter the domain horizontally in order to avoid the vertical acceleration which generated by chimney effects, Bello-Ochende T. and Bejan A.,(2005), [8].

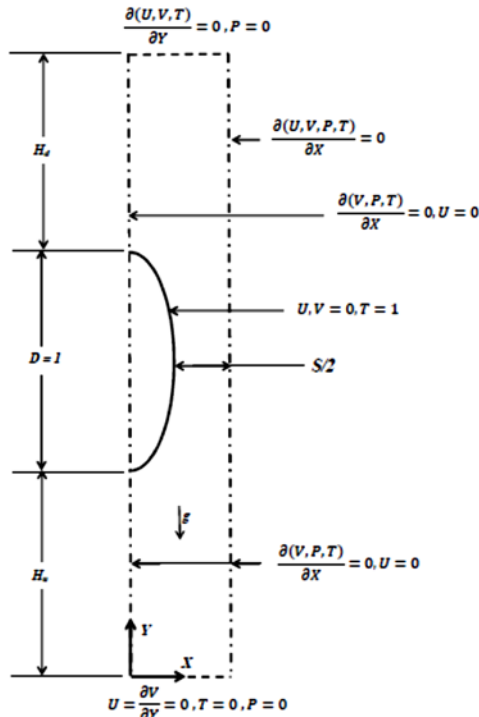


Figure (2): Dimensionless Boundary Conditions on the Flow Channel

3. Optimization of Heat Transfer (Maximum Heat Transfer Density)

The spacing between the tubes is to be chosen such that the heat transfer density (objective function) is maximized. The heat transfer density is the heat transfer rate per unit volume and given as;

$$q''' = \frac{q}{V} = \frac{q}{(s + 2b)dw} = \frac{q'}{(s + 2b)d} \quad (6)$$

Where q' = Total heat transfer rate from one tube per unit width.

The heat transfer density can be written in non-dimensional form as;

$$Q = \frac{q' d^2}{k (T_w - T_\infty)(s + 2b)d} \quad (7)$$

$$Q = \frac{-\left(\int_0^d k \frac{\partial T}{\partial x} dy\right) d}{k(T_w - T_\infty)(s + 2b)} = \frac{-\int_0^1 \frac{\partial T}{\partial X} dY}{(S + 2\varepsilon)} \quad (8)$$

The objective function (heat transfer density) subjected to the constraint that the total volume per unit width is fixed.

$$\therefore (dL) = \text{Constant} \quad (9)$$

4. Numerical Procedure, Grid Independence Test, and Validation

A FORTRAN program is written to solve the algebraic equations which obtained by the finite volume method. The general transport equation is firstly transformed to curvilinear coordinates and the convective term is discretized by hybrid scheme while the diffusion term is discretized by second order central scheme. For coupling between the pressure and velocity SIMPLE algorithm is employed. To prevent the oscillation in the pressure field the interpolation method of Rhie, C. M., and Chow, W. L., (1983), [12], is used. The solution algorithm can be summarized as;

- 1- Solve the discretized momentum equations to find the velocity field.
- 2- Solve the pressure correction equation to find the corrected pressure.
- 3- Correct the velocity field by using the corrected pressure.
- 4- Solve the discretized energy equation to find the temperature.
- 5- Repeat the steps (1-4) until convergence attained.

The grid independence test is performed for three grids for configuration at which ($Ra = 10^4$, $\varepsilon = 0.1$, and $S = 0.3$). The grid independence test showed that the increasing of the grid size decreases the error percentage, and the minimum error is at 50×50 control volumes per (D). So this grid size is used and adopted in all results. Grid independence test is illustrated in table (1). To apply the correct velocity and temperature at the inlet and outlet of the channel, the upstream extension (H_u) is added at the inlet of the channel and downstream extension (H_d) is added at the outlet of the channel. It is observed from the table (2) for ($Ra = 10^5$, $\varepsilon = 0.1$, and $S = 0.1$) that the increasing in downstream extension to ($H_d = 2$) and keeping the upstream at ($H_u = 0.5$) leads to reduce the error in the heat transfer density to 2.5%. Based on this test the value of ($H_u = 0.5$) and ($H_d = 2$) have been depended in all numerical results.

The numerical results are validated by comparing the results of (S_{opt}) with the numerical results of Da Silva and Bejan, (2004), [4] for natural convection between vertical isothermal plates ($\varepsilon = 0$) and with Bello-Ochende and Bejan, (2005), [8] for natural convection between isothermal cylinders ($\varepsilon = 0.5$). Both comparisons are carried out at ($Ra = 10^5$). Good agreement can be shown in table (3) for both cases.

Table 1: Grid Independence Test for the Case ($Ra = 10^4$, $\varepsilon=0.1$, and $S=0.3$)

Number of Control Volumes Per D	Q	Error%
30 x 30	30.94532	-----
40 x 40	31.41611	0.69
50 x 50	31.21666	0.63

Table 2: Downstream Extension Test for the Case ($Ra = 10^5$, $\varepsilon=0.25$, $H_u=0.5$ and $S=0.1$)

H_d	Q	Error %
0.5	31.27484	-----
1	32.50780	3.94
1.5	33.41908	2.8
2	34.26481	2.5

Table 3: Comparison of the Numerical Results for (S_{opt}) with the Previous Results for Case $Ra=10^5$ ($\varepsilon = 0$, and $\varepsilon=0.5$)

Flat Plate ($\varepsilon=0$)		
Da Silva A.K., and Bejan A. (2004), [4]		Present
0.129		0.13
Circular Tube ($\varepsilon=0.5$)		
Bello-Ochende T., and Bejan A., (2005), [8]		Present
0.104		0.12

5. Results and Discussion

The numerical results are presented in this section for, temperature contours, optimal spacing, and density of heat transfer for different values of tube axis ratio ($0 \leq \varepsilon \leq 0.5$). The range of Rayleigh number is ($10^3 \leq Ra \leq 10^5$) and the working fluid is air with ($Pr=0.71$).

Figure (3) shows the temperature contour as a function of the spacing between the tubes (S) for ($Ra=10^3$) and axis ratio ($\varepsilon = 0.1$). For small spacing ($S \leq 0.25$) the downstream region is occupied by hot fluid at temperature same as the wall temperature (red region), this is due to that the small spacing between the tubes prevents the cold air to flow downstream and the air there still hot (overworked fluid). As the spacing between the tubes increases ($S \geq 0.25$) the downstream temperature begins to decrease and become less than the wall temperature and this is clear from the appearance of the (orange, yellow and green) regions. At some spacing the thermal boundary layers from both sides are merged at the downstream region (the channel is fitted with the convective flow body) , at this spacing the heat transfer density becomes maximum and the spacing represents the optimal spacing, in this case ($S_{opt} = 0.41$). Further increasing in spacing between the tubes leads to a cold fluid region to appear in the downstream as seen in the blue region (underworked fluid) for ($S \geq 1$), this large spacing permits the ambient (cold) fluid to flow downstream and leads to decrease the heat transfer density since the

thermal conductance between the tubes decreased.

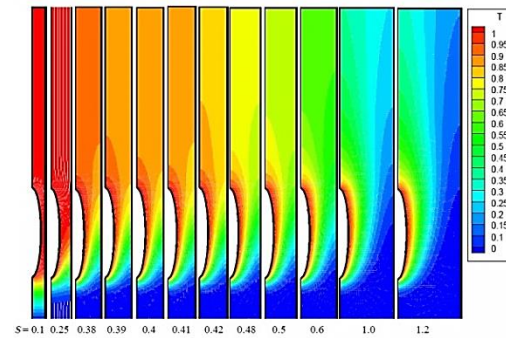


Figure (3): Temperature contour with various spacing between the tube for ($Ra=10^3$, $Pr =0.7$, and axis ratio $\varepsilon=0.1$)

As Rayleigh number increases to ($Ra=10^4$) same behavior of the temperature contour to that of ($Ra=10^3$) as can be observed in figure (4) except that the optimal spacing here becomes smaller, note that ($S_{opt} = 0.41$ at $Ra=10^3$) while ($S_{opt} = 0.22$ at $Ra=10^4$), so as Rayleigh number increases the optimal spacing decreases because the thermal boundary layer thickness decreases with increasing of Rayleigh number, this is also obvious from the temperature contour for ($Ra=10^5$) in figure (5) in which the optimal spacing is ($S_{opt} = 0.12$) while the optimal spacing for ($Ra=10^4$) is (0.22).

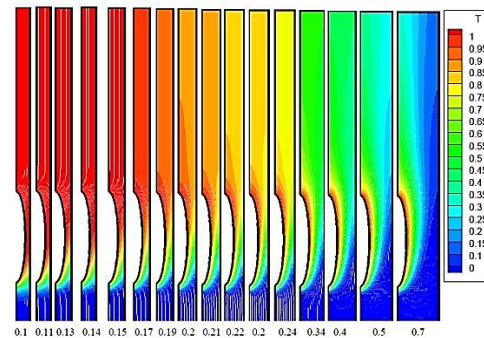


Figure (4): Temperature contour with various spacing between the tube for ($Ra=10^4$, $Pr =0.7$, and axis ratio $\varepsilon=0.1$)

Figures (6, 7, and 8) illustrate the temperature contours at ($\varepsilon = 0.25$) and for Rayleigh numbers (10^3 , 10^4 , and 10^5), respectively. The temperature contours are similar to that of ($\varepsilon=0.1$) at the same Rayleigh number.

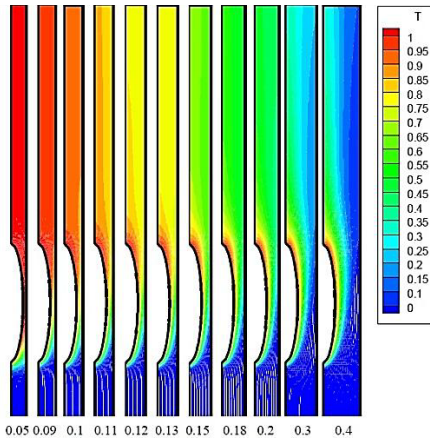


Figure (5): Temperature contour with various spacing between the tube for ($Ra=10^5$, $Pr=0.7$, and axis ratio $\varepsilon=0.1$)

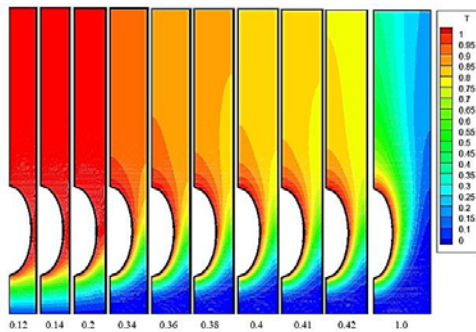


Figure (6): Temperature contour with various spacing between the tube for ($Ra=10^3$, $Pr=0.7$, and axis ratio $\varepsilon=0.25$)

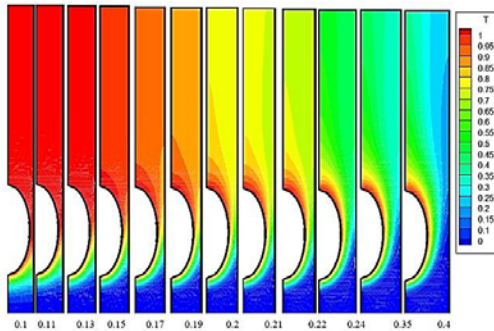


Figure (7): Temperature contour with various spacing between the tube for ($Ra=10^4$, $Pr=0.7$, and axis ratio $\varepsilon=0.25$)

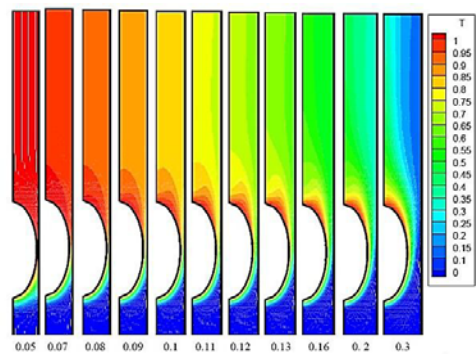


Figure (8): Temperature contour with various spacing between the tube for ($Ra=10^5$, $Pr=0.7$, and axis ratio $\varepsilon=0.25$)

Figures (9, and 10) show the dimensionless heat transfer density as a function of the spacing at different Rayleigh numbers and for ($\varepsilon=0.1$, and 0.25) respectively. These figures show that there is optimal spacing for each Rayleigh number. At this value of spacing the heat transfer density reaches its maximum value (tops of the curves).

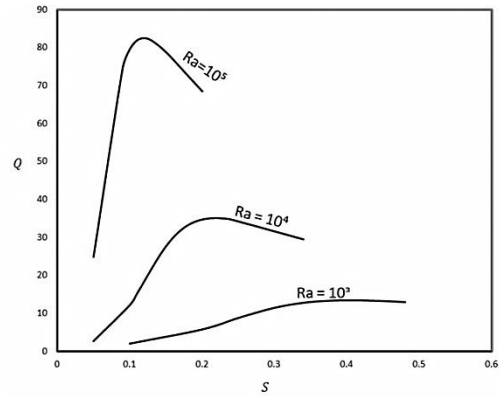


Figure (9): Heat Transfer Density with spacing at different Rayleigh numbers for axis ratio ($\varepsilon=0.1$)

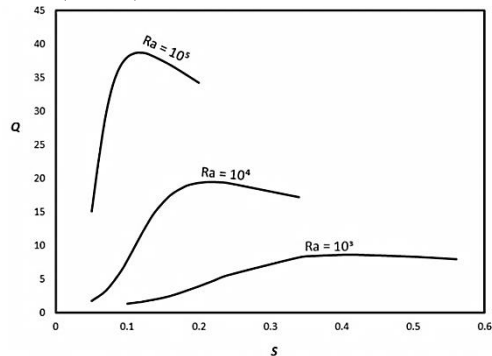


Figure (10): Heat Transfer Density with spacing at different Rayleigh numbers for axis ratio ($\varepsilon=0.25$)

Figure (11) shows the optimal spacing (S_{opt}) versus Rayleigh number at various axis ratio ($\varepsilon=0, 0.25$, and 0.5), it is interesting to note that the optimal spacing decreases as Rayleigh number increases for all values of (ε), as mentioned above the increasing of Rayleigh number reduces the thermal boundary layer thickness and thus the optimal spacing decreased.

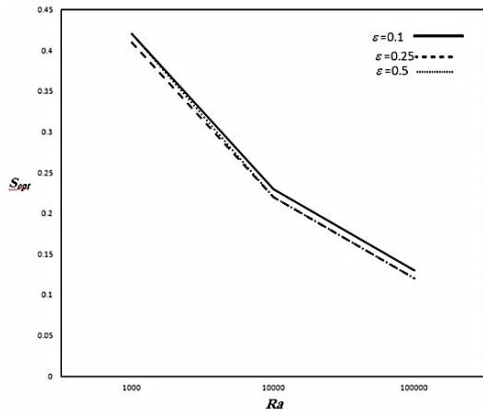


Figure (11): Optimal spacing with Rayleigh number for different axis ratios

Figure (12) shows the maximum heat transfer density versus Rayleigh number at various axis ratio (ϵ), it can be noted that the maximum heat transfer density increases as Rayleigh number increases for all values of (ϵ), the increasing of Rayleigh number leads to increase the buoyancy force and thus increase the maximum heat transfer density. It also can be seen that the highest value of the maximum heat transfer density occurs at ($\epsilon = 0$, flat plate) and decreases as the axis ratio increases until reaches the lowest value at ($\epsilon = 0.5$, circular plate). This can be explained as the axis ratio increases (the curvature of the surface increases) the temperature gradient near the wall decreases and thus the maximum heat transfer density decreases.

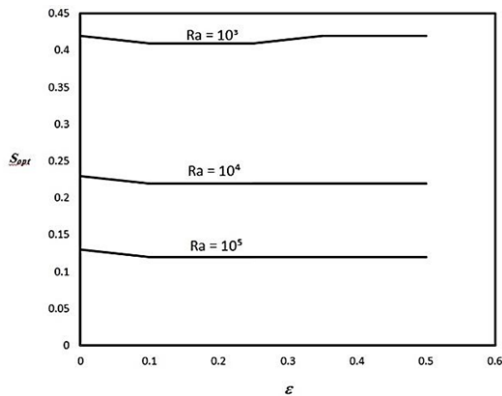


Figure (12) Maximum heat transfer density with Rayleigh number for different axis ratios.

Figure (13) shows the optimal spacing versus the axis ratio of the tube at different Rayleigh numbers. The optimal spacing is almost constant for all values of the axis ratio. Since the optimal spacing is nearly constant for all (ϵ), the number of tubes installed in the same volume must be reduced as the axis ratio increases.

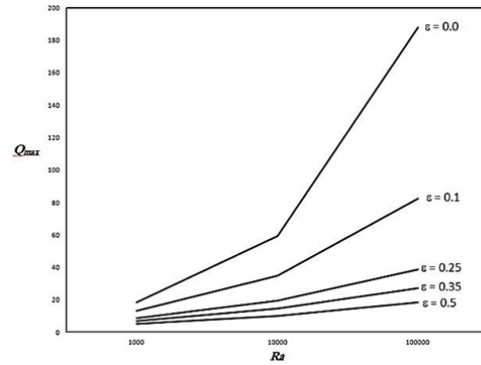


Figure (13): Optimal spacing with different axis ratios for Rayleigh number.

6. Conclusions

The conclusions for optimal spacing between elliptic tubes cooled by natural convection can be summarized as:-

- 1- The optimal spacing decreases as Rayleigh number increases for all axis ratios. The maximum heat transfer increases as Rayleigh number increases for all axis ratios.
- 2- The highest value of the maximum heat transfer density occurs at axis ratio ($\epsilon = 0$, flat plate) and lowest value occurs at axis ratio ($\epsilon = 0.5$, circular plate) for all Rayleigh numbers.
- 3- The optimal spacing remains constant as the axis ratio increases at constant Rayleigh number.
- 4- The number of tubes installed in the same volume must be reduced as the axis ratio increases.

7. References

- 1- Bejan A. and Lorente S., Design with Constructal Theory, Wiley, New York, 2008.
- 2- Bejan A., Convection Heat Transfer, Wiley, New York, 1984.
- 3- Bejan A., Fowler A.J., and Stanescu G., The optimal spacing between horizontal cylinders in a fixed volume cooled by natural convection, International Journal of Heat and Mass Transfer 38, 2047–2055, 1995.
- 4- Ledezma G. A., and Bejan A., Optimal Geometric Arrangement of Staggered Vertical Plates in Natural Convection, Journal of Heat Transfer, 119, 700-708, 1997.
- 5- Da Silva A.K., Bejan A., Maximal Heat Transfer Density in Vertical Morphing Channels with Natural Convection, Numerical Heat Transfer, Part A, 45: 135-152, 2004

- 6- Da Silva A.K., and Bejan A., Constructal multi-scale structure for maximal heat transfer density in natural convection, Int. J. Heat Fluid Flow 26, 34–44, 2005.
- 7- Da Silva A.K., Lorenzini G., and Bejan A., Distribution of heat sources in vertical open channels with natural convection, International Journal of Heat and Mass Transfer 48, 1462-1469, 2005.
- 8-Bello-Ochende T., and Bejan A., Constructal multi-scale cylinders with natural convection, International Journal of Heat and Mass Transfer 48, 4300–4306, 2005.
- 9- Page L., Bello-Ochende T., and Meyer J., Maximum heat transfer density rate enhancement from cylinders rotating in natural convection, Int. Commun. Heat Mass Transfer 38, 1354–1359, 2011.
- 10- Page L., Bello-Ochende T., and Meyer J., Constructal multi scale cylinders with rotation cooled by natural convection, International Journal of Heat and Mass Transfer 57, 345–355, 2013.
- 11- Zhang Z., Bejan A., and Lage J.L., Natural Convection in a Vertical Enclosure with Internal Permeable Screen, Journal of Heat Transfer, 113, 377-383, 1991.
- 12- Rhie, C. M., and Chow, W. L., Numerical Study of the Turbulent Flow Past an Airfoil with Trailing Edge Separation , AIAA Journal, 21, 1525-1532, 1983.

البعد الامثل بين انابيب بيضوية مبردة بالحمل الحر باستخدام نظرية التشبيد

أحمد وحيد مصطفى

جامعة النهريين – كلية الهندسة قسم الهندسة الميكانيكية

جعفر احمد زاهي

جامعة النهريين – كلية الهندسة قسم الهندسة الميكانيكية

الخلاصة

البعد الامثل بين انابيب بيضوية مبردة بالحمل الطبيعي درس عدديا. صف من الانابيب البيضوية ثابتة درجة الحرارة نصبت في حجم محدد والبعد بينهم اختير بموجب نظرية التشبيد (نظرية بيجان). في هذه النظرية البعد اختير بحيث تكون كثافة انتقال الحرارة اقصى ما يمكن. طريقة الحجم المحدد استخدمت لحل المعادلات الحاكمة، خوارزمية SIMPLE مع شبكة متحدة الموقع استخدمت للربط بين السرعة والضغط. مدى رقم رايلي $(10^3 \leq Ra \leq 10^5)$ ومدى نسبة الاحداثي للانابيب $(0 \leq \epsilon \leq 0.5)$ ومائع التشغيل هو الهواء ($Pr=0.7$). بينت النتائج ان البعد الامثل يقل مع زيادة رقم رايلي لكل نسب الاحداثيات وكثافة انتقال الحرارة العظمى تزداد مع زيادة رقم رايلي لكل نسب الاحداثي وقيمتها العليا تحدث عند نسبة احداثي $(\epsilon=0)$ ، صفيحة مستوية) وقيمتها السفلى تحدث عند نسبة احداثي $(\epsilon=0.5)$ ، انبوب دائري). بينت النتائج ايضا ان البعد الامثل لا يتغير مع نسبة الاحداثي عند رقم رايلي ثابت.